

Spin motion of photoelectrons

J. Henk,* P. Bose, Th. Michael, and P. Bruno

Max-Planck-Institut für Mikrostrukturphysik, Weinberg 2, D-06120 Halle (Saale), Germany

(Received 16 May 2003; published 12 August 2003)

Ab initio and model calculations demonstrate that the spin motion of electrons transmitted above the vacuum energy through ferromagnetic films can be investigated by means of angle- and spin-resolved core-level photoelectron spectroscopy. The motion of the photoelectron spin polarization can be regarded as a combination of a precession around and a relaxation towards the magnetization direction. For ultrathin Fe films on Pd(001), its dependence on the Fe film thickness and on the Fe electronic structure is studied systematically. In addition to elastic and inelastic scattering, the effect of band gaps on the spin motion is addressed in particular.

DOI: 10.1103/PhysRevB.68.052403

PACS number(s): 75.70.Ak, 79.60.-i, 73.40.Gk, 75.50.Bb

Taking advantage of the spin in electronic devices, in order to form new “spintronic” devices, is currently in progress worldwide. This goal challenges both applied and basic physics, the latter being mostly concerned with model systems of spin-dependent transport.¹ Aiming at very small devices, the properties of magnetic nanostructures become increasingly important. In particular, spin-dependent scattering in ultrathin films and at interfaces may have a profound effect on the transport properties^{2,3}: the electronic spins start to precess and the spin current applies a spin-transfer torque on the magnetization in the ferromagnet. To understand in detail the spin motion in electron transmission through magnetic films, one obviously needs a microscopic probe.

Ferromagnetic resonance, used successfully to study the magnetic properties of multilayer systems,⁴ cannot deal with electron transmission. However, spin- and time-resolved photoelectron spectroscopy was employed to investigate directly spin filtering in the time domain.⁵ Spin motion, which can be regarded as a combination of a precession of the electron spin polarization (ESP) \vec{P} around the magnetization direction and as relaxation of \vec{P} towards the magnetization \vec{M} , is interesting in its own right.^{6,7} A successful method which addresses the spin motion of electrons above the vacuum level is the transmission of spin-polarized electrons (usually produced with a GaAs source) through freestanding ferromagnetic films.⁸ Further, spin motion was recently observed in spin-resolved low-energy electron diffraction (SPLEED).⁹

The purpose of this paper is twofold. First, we propose to apply angle- and spin-resolved photoelectron spectroscopy from core levels to access directly the spin motion of electrons transmitted through an ultrathin ferromagnetic film (Fig. 1). Therefore, it is proved by means of *ab initio* calculations that precession and relaxation can be observed in experiments. We are not aware of other first-principles investigations of spin motion in electron transmission. Beyond that, it is shown that spin motion can serve as a tool for obtaining information on the electronic and magnetic structure of the system.

Our approach relies in particular on the possibility to orient the spin polarization of the incoming photoelectrons by the incident light, an effect due to spin-orbit coupling. In the following, the basic ideas are described for the chosen systems n monolayer (ML) Fe/Pd(001), $n = 1, \dots, 6$ (for details, see Ref. 10).

(i) The incident light excites electrons from Pd $3d_{3/2}$ core levels of the Pd(001) substrate into a state above the vacuum level E_{vac} .

(ii) Choosing linearly p -polarized light with incidence direction given by $\vartheta_{\text{ph}} = 45^\circ$ polar angle and variable azimuth φ_{ph} , the ESP in the substrate can be aligned to any desired direction in the xy surface plane (Cartesian coordinates are defined in Fig. 1). It was theoretically and experimentally shown for nonmagnetic layered systems with fourfold rotational symmetry that an ESP perpendicular to the scattering plane (spanned by the surface normal and the incidence direction; see Ref. 11 and references therein) is produced: $\vec{P}^{\text{in}} \propto (-\sin \varphi_{\text{ph}}, \cos \varphi_{\text{ph}}, 0)$. For $\varphi_{\text{ph}} = 0^\circ$ and 180° , \vec{P}^{in} is perpendicular to the magnetization \vec{M} (which is parallel to x). Hence, the commonly used external GaAs source for spin-polarized electrons is, so to speak, replaced by an internal one, with the advantage of easy orientation of \vec{P}^{in} .

(iii) During the transmission through the Fe film, the photoelectron is subject to elastic and inelastic scattering processes. Both can simply be modeled by spin-dependent scattering at an asymmetric quantum well which comprises the substrate-film and film-vacuum interfaces. The transmitted ESP \vec{P}^{tr} reads

$$\vec{P}^{\text{tr}} \propto \begin{pmatrix} |T^\uparrow|^2 - |T^\downarrow|^2 + P_x^{\text{in}}(|T^\uparrow|^2 + |T^\downarrow|^2) \\ P_y^{\text{in}} \text{Re}(T^\uparrow T^\downarrow) - P_z^{\text{in}} \text{Im}(T^\uparrow T^\downarrow) \\ P_z^{\text{in}} \text{Re}(T^\uparrow T^\downarrow) + P_y^{\text{in}} \text{Im}(T^\uparrow T^\downarrow) \end{pmatrix}, \quad (1)$$

where the spin-dependent transmission coefficients $T^{\uparrow(\downarrow)}$ take into account multiple reflection. Considering elastic scattering, the dependence of \vec{P}^{tr} on the film thickness d shows two oscillation periods. The precession of the transversal components P_y^{tr} and P_z^{tr} around \vec{M} (Refs. 12 and 13) has a longer period with wavelength $2\pi/(k_z^\uparrow - k_z^\downarrow)$, $k_z^{\uparrow(\downarrow)}$ being the electron wave numbers in the film. Multiple reflection at the interfaces results in a short-period oscillation with wavelength $2\pi/(k_z^\uparrow + k_z^\downarrow)$ and much smaller amplitude. The longitudinal component P_x^{tr} remains constant on average.

Inelastic scattering leads to spin-dependent attenuation within the film. Simulated by multiplying the propagators between the interfaces by $\exp(-d/\lambda^{\uparrow(\downarrow)})$, this spin-filter effect relaxes \vec{P}^{tr} towards \vec{M} (i.e., $\lim_{d \rightarrow \infty} P_x^{\text{tr}} = 1$ for $\lambda^\uparrow > \lambda^\downarrow$). It

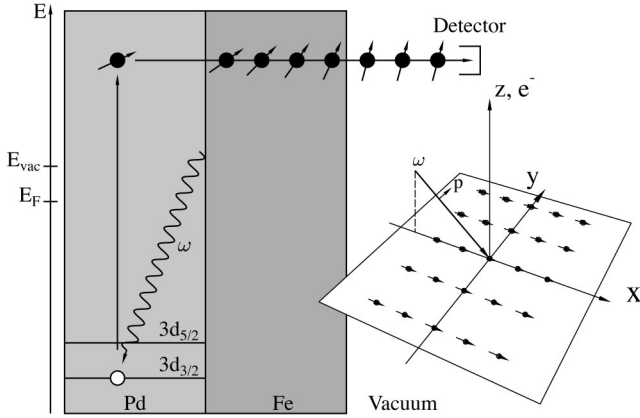


FIG. 1. Spin motion in electron transmission through a ferromagnetic film accessed by photoelectron spectroscopy. Left: a core electron is excited by the incident radiation (wavy line, photon energy ω) in the Pd substrate (light gray). The spin polarization (arrow) of the photoelectron (solid circle) is oriented due to spin-orbit interaction. During the transmission through the magnetic Fe film (dark gray), the spin polarization rotates further (spin motion) but stops rotating in the vacuum. E_F and E_{vac} are the Fermi and vacuum levels, respectively. Right: setup of normal photoemission from a ferromagnetic surface (with magnetization along x) and p -polarized light incident in the xz plane.

was successfully used to determine the attenuation lengths $\lambda^{\uparrow(1)}$ (Refs. 14 and 15) and to obtain the spin-resolved electronic structure of Fe.¹⁶ There is no spin motion in nonmagnetic regions (e.g., vacuum).

(iv) The photoelectrons are eventually detected as spin resolved in normal emission ($\vec{k}_{\parallel}=0$). The electron energies are considerably larger than those in spin-dependent transport measurements. To come closer to the Fermi level one might use threshold photoemission (PE) or deposit a work-function-reducing adlayer onto the surface.

The small photoelectron escape depth^{17,18} restricts d to a few ML. This implies for ultrathin films that the short-period oscillation might dominate the spin motion, a complete precession cannot be observed, and the relaxation limit ($\vec{P}_{\parallel}\vec{M}$) cannot be reached in practice. The present approach is not restricted to linearly polarized light. Spectra for circularly polarized light (not reported here), for which one can produce \vec{P}^{in} with a component along the surface normal,¹⁹ agree qualitatively with those discussed here.

Theoretical. To obtain reliable results, we rely on a computational scheme which proved to be successful in describing qualitatively and quantitatively PE from nonmagnetic and ferromagnetic surfaces in the valence-band and core-level regimes (Ref. 20 and references therein). Starting from first-principles electronic-structure calculations for 0–6 ML fcc Fe/Pd(001) [Ref. 10, local spin-density approximation of density-functional theory, screened Korringa-Kohn-Rostoker (KKR) method; for details, see Ref. 21], spin- and angle-resolved constant-initial-state PE spectra were computed within the relativistic one-step model (layer-KKR method; cf. Ref. 22). The latter describes PE correctly as a coherent process (in contrast to the three-step model which treats excitation, propagation towards the surface, and transmission

into the vacuum separately). The applicability of the initial-state picture of core-level PE (see, e.g., Ref. 20) was checked by comparing theoretical with experimental spectra. Here, a poor description would affect mainly the size of the incoming ESP. The general results on spin motion, however, would still be valid. Within the KKR method, the semi-infinite systems (Pd substrate/Fe film/vacuum) were treated with the correct boundary conditions. Reasonable values were chosen for the free parameters¹⁰; e.g., the first 30 layers contributed to the photocurrent.

The structure of Fe on Pd(001) depends on the preparation conditions and can show disorder and imperfections at the surface.²³ Since the present investigation focuses on the basic spin-motion effects, we deliberately choose ideal fcc Fe films instead. Consequently, a perfect agreement with future experiments is not expected.

We choose Fe/Pd(001) due to the large magnetic moment of Fe and the strong spin-orbit coupling in Pd which results in a sizable \vec{P}^{in} . The covering Fe induces a magnetic moment of about $0.24\mu_B$ in the Pd layer close to the Fe/Pd interface.¹⁰ Hence, \vec{P}^{in} originates from the induced exchange splitting and from spin-orbit coupling. That the spin motion is dominantly due to the Fe magnetism was checked by considering several “artificial” magnetic configurations and by variation of the azimuth of light incidence. Further, changing the inverse photoelectron lifetime in the Fe film allowed us to differentiate between elastic (precession around \vec{M}) and inelastic processes (relaxation towards \vec{M}).

Elastic and inelastic processes. Inelastic processes can be simulated in calculations by adding an imaginary self-energy to the potential (see, e.g., Ref. 24). To unveil the influence of these processes, the inverse photoelectron lifetime in the Fe film was reduced to 0.001 eV (“elastic” case), as compared to the otherwise chosen 1.8 eV (“inelastic” case). Being rather small and almost constant in the elastic case, P_x^{tr} in-

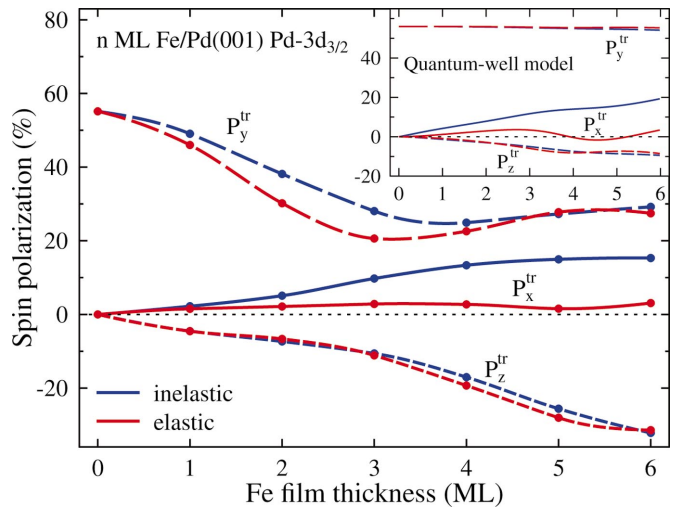


FIG. 2. (Color) Elastic and inelastic effects in spin motion for 0–6 ML Fe on Pd(001) at 17.5 eV kinetic energy and azimuth of light incidence $\varphi_{ph}=0^\circ$. The transmitted electron-spin polarization \vec{P}^{tr} is shown vs Fe-film thickness n (in ML) for the inelastic (blue) and elastic (red) cases. The inset shows corresponding results of a model calculation.

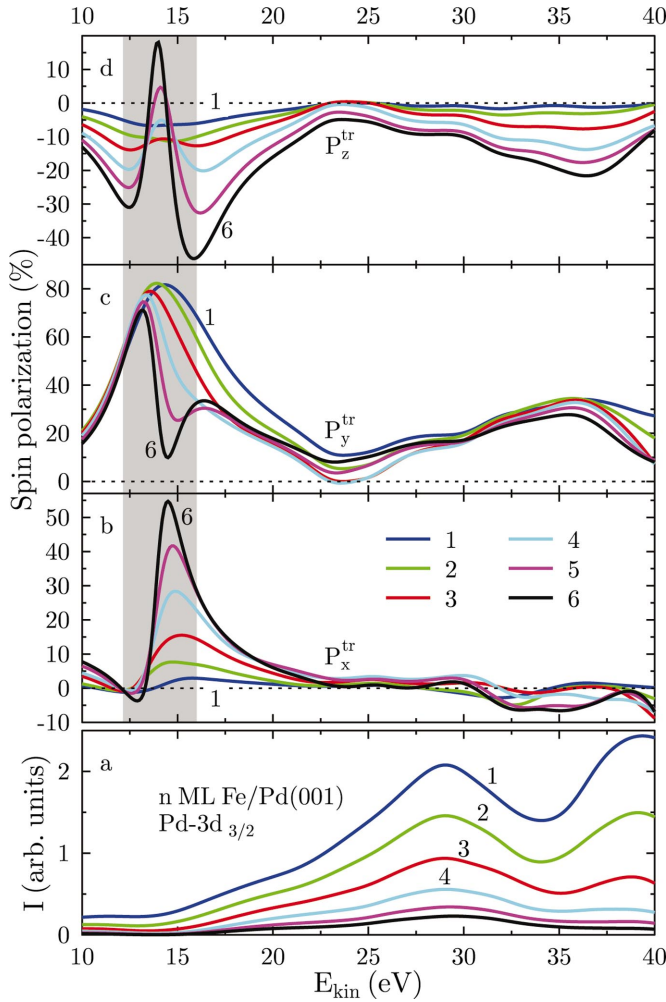


FIG. 3. (Color) Energy dependence of the spin motion for 1–6 ML Fe on Pd(001). (a) Spin-averaged constant-initial-state photoemission intensities I vs kinetic energy E_{kin} of the photoelectrons. (b)–(d) Transmitted electron-spin polarization \vec{P}^{tr} . The Fe-film thickness n (in ML) is indicated by numbers and color coding. The gray area highlights a prominent feature discussed in the text.

increases with Fe coverage in the inelastic case (Fig. 2), i.e., \vec{P}^{tr} starts to relax towards \vec{M} . Because the short-period oscillation is relevant for ultrathin films, the precession of \vec{P}^{tr} around \vec{M} (which shows the long wavelength) cannot be clearly observed. To corroborate these findings, we calculated \vec{P}^{tr} within the quantum-well model sketched preceding, with parameters obtained from the Pd and Fe bulk-band structures (inset in Fig. 2). The resulting wavelengths of about 200 ML (precession) and 3.9 ML (multiple reflection) lead to reasonable agreement concerning P_x^{tr} and P_z^{tr} . However, P_y^{tr} does not show such a pronounced minimum at 3–4 ML. The differences between model and *ab initio* calculations can be attributed to the number of transmission channels: a single one in the model but several channels (with different wavelengths) in the *ab initio* calculations.

Effects of the electronic structure. To show how the spin motion depends on details of the electronic structure, we address constant-initial-state PE spectra. In contrast to

SPLEED experiments in which \vec{P}^{in} is typically parallel or antiparallel to the magnetization,^{25,26} a transverse \vec{P}^{in} ($\varphi_{\text{ph}} = 0^\circ$) is chosen. For clarity reasons, the following discussion rests upon the complex bulk-band structure, rather than on layer-resolved spectral densities. The “pure” effect is worked out by a model calculation, rather than complicating the discussion by complex-band structures.

The spin-averaged intensities [Fig. 3(a)] decrease significantly with Fe coverage, caused by the small photoelectron escape depth. The global shape of the spectra, however, remains almost unaffected. Changes of the slopes, best to be seen for 1 ML Fe but present for all Fe-film thicknesses, can be traced back to the Fe electronic structure (not shown): an increase of the slope is associated with the onset of additional transmission channels, i.e., dispersive Fe bands. In particular, one pair of spin-split bands provides efficient transmission, which leads to the intensity increase at about 15 eV. A Pd-band gap, which reduces the number of channels in the substrate, causes the pronounced minimum at about 34 eV kinetic energy.

At low energies where the number of transmission channels is small, the evolution of \vec{P}^{tr} with Fe coverage is almost monotonous [Figs. 3(b)–3(d)]. The most significant structures show up between 12 eV and 16 eV (gray area): P_x^{tr} and P_y^{tr} display $-/+$ and $+/-$ modulations, respectively, accompanied by a maximum in P_z^{tr} . A detailed analysis corroborates their relation to the Fe electronic structure, in particular to exchange-split band gaps in conjunction with the onset of additional transmission channels in that particular energy range.

To provide direct evidence that band gaps manifest themselves pronounced in spin motion, the ESP is calculated in an inelastic three-band nearly-free-electron model. The substrate is taken as semi-infinite free space (with zero potential), whereas a nonzero scattering potential in the magnetic film gives rise to exchange-split band gaps [Figs. 4(a) and 4(b)]. There, the transmission of one spin channel is reduced

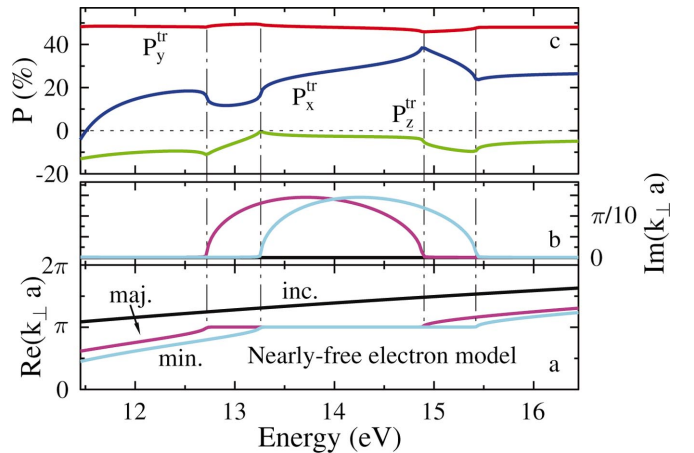


FIG. 4. (Color) Effect of exchange-split band gaps in the film electronic structure on the spin motion. (a) and (b) Complex band structure of the substrate (“inc.,” black) and the magnetic film (majority, “maj.,” magenta; minority, “min.,” cyan) in the extended zone scheme. (c) Electron spin polarization of the transmitted electrons. Vertical dash-dotted lines serve as guides to the eye.

due to evanescent states [nonzero $\text{Im}(k_z)$ in Fig. 4(b)]. Since incoming transverse spinors are weighted sums of spin-up (“maj.”) and spin-down (“min.”) Pauli spinors ($P_y^{\text{in}} = 50\%$), P_x^{tr} and P_y^{tr} show a $-/+$ and a small $+/-$ modulation, respectively, whereas P_z^{tr} increases in the band-gap middle [Fig. 4(c)]. Although the Fe-band structure is much more complicated, the structures in the model calculation have counterparts in Figs. 3(b)–3(d) (gray area). Distinct band-gap related features do not show up at higher kinetic energies due to the onset of several efficient transmission channels just at about 15 eV.

Conclusions. First-principles “theoretical experiments” demonstrate that the spin motion in electron transmission

through ferromagnetic films can be analyzed in detail by angle- and spin-resolved photoelectron spectroscopy. Calculations for Fe films on Pd(001), which are to be confirmed experimentally, suggest promising analyses of spin-dependent transport through magnetic layers. In particular, information on the electronic and magnetic film structure is obtained since intensities and spin polarizations depend significantly on the film thickness. Beyond that, one can speculate to use the approach for investigating magnetic configurations, with the possibility of analyzing noncollinear magnetism. The main advantages appear to be that the preparation of freestanding films is avoided and that the spin polarization of the incoming electrons can easily be oriented.

*Corresponding author. Electronic address: henk@mpi-halle.de

¹*Spin Dependent Transport in Magnetic Nanostructures*, edited by S. Maekawa and T. Shinjo (Taylor & Francis, London, 2002).

²S.S.P. Parkin, *J. Appl. Phys.* **79**, 6078 (1996).

³P. Zahn, J. Binder, I. Mertig, R. Zeller, and P.H. Dederichs, *Phys. Rev. Lett.* **80**, 4309 (1998).

⁴J.A.C. Bland and B. Heinrich, *Ultrathin Magnetic Structures* (Springer, Berlin, 1994).

⁵M. Aeschlimann, R. Burgermeister, S. Pawlik, M. Bauer, D. Oberli, and W. Weber, *J. Electron Spectrosc. Relat. Phenom.* **88-91**, 179 (1998).

⁶D. Oberli, R. Burgermeister, S. Riesen, W. Weber, and H.C. Siegmann, *Phys. Rev. Lett.* **81**, 4228 (1998).

⁷W. Weber, D. Oberli, S. Riesen, and H.C. Siegmann, *New J. Phys.* **1**, 9.1 (1999).

⁸Y. Lassailly, H.-J. Drouhin, A.J. van der Sluijs, and G. Lampel, *Phys. Rev. B* **50**, 13 054 (1994).

⁹W. Weber, S. Riesen, C.H. Back, A. Shorikov, V. Anisimov, and H.C. Siegmann, *Phys. Rev. B* **66**, 100405(R) (2002).

¹⁰J. Henk and A. Ernst, *J. Electron Spectrosc. Relat. Phenom.* **125**, 107 (2002).

¹¹J. Henk, T. Scheunemann, and R. Feder, *J. Phys.: Condens. Matter* **9**, 2963 (1997).

¹²M.D. Stiles and A. Zangwill, *J. Appl. Phys.* **91**, 6812 (2002).

¹³M.D. Stiles and A. Zangwill, *Phys. Rev. B* **66**, 014407 (2002).

¹⁴D.P. Pappas, K.-P. Kämper, B.P. Miller, H. Hopster, D.E. Fowler, C.R. Brundle, A.C. Luntz, and Z.-X. Shen, *Phys. Rev. Lett.* **66**, 504 (1991).

¹⁵M.P. Gokhale and D.L. Mills, *Phys. Rev. Lett.* **66**, 2251 (1991).

¹⁶W. Kuch, M.-T. Lin, K. Meinel, C.M. Schneider, J. Noffke, and J. Kirschner, *Phys. Rev. B* **51**, 12 627 (1995).

¹⁷M.P. Seah and W.A. Dench, *Surf. Interface Anal.* **1**, 2 (1979).

¹⁸A. Jablonski and C.J. Powell, *Surf. Sci. Rep.* **47**, 33 (2002).

¹⁹J. Henk, T. Scheunemann, S.V. Halilov, and R. Feder, *J. Phys.: Condens. Matter* **8**, 47 (1996).

²⁰J. Henk, A.M.N. Niklasson, and B. Johansson, *Phys. Rev. B* **59**, 13 986 (1999).

²¹A. Ernst, M. Lüders, W.M. Temmerman, Z. Szotek, and G. van der Laan, *J. Phys.: Condens. Matter* **12**, 5599 (2000).

²²J. Henk, in *Handbook of Thin Film Materials*, edited by H.S. Nalwa (Academic Press, San Diego, 2001), Vol. 2, Chap. 10, p. 479.

²³S.-K. Lee, J.-S. Kim, B. Kim, Y. Cha, W.K. Han, H.G. Min, J. Seo, and S.C. Hong, *Phys. Rev. B* **65**, 014423 (2002).

²⁴J. Rundgren, *Phys. Rev. B* **59**, 5106 (1999).

²⁵T. Scheunemann, R. Feder, J. Henk, E. Bauer, T. Duden, H. Pinkvos, H. Poppa, and K. Wurm, *Solid State Commun.* **104**, 787 (1997).

²⁶S. Egger, C.H. Back, J. Krewer, and D. Pescia, *Phys. Rev. Lett.* **83**, 2833 (1999).